Food Chemistry: X 22 (2024) 101260

Contents lists available at ScienceDirect

Food Chemistry: X

journal homepage: www.sciencedirect.com/journal/food-chemistry-x

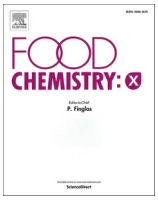

Fabrication and characterization of salidroside W/O/W emulsion with sodium alginate

Qian Zhang [a], Yu-Qiao Wang [b], Lin Li [b], Hao-Lin Song [b], Hai-Tao Wu [b,*], Bei-Wei Zhu [a,b,*]

[a] College of Food Science and Engineering, Jilin University, Changchun, Jilin 130062, China
[b] SKL of Marine Food Processing & Safety Control, National Engineering Research Center of Seafood, Collaborative Innovation Center of Seafood Deep Processing, School of Food Science and Technology, Dalian Polytechnic University, Dalian 116034, China

ARTICLE INFO

Keywords:
Salidroside
W/O/W emulsion
Sodium alginate
Storage stability

PubChem studied in this article:
Salidroside (PubChem CID: 159278)
Sodium alginate (PubChem CID: 133126842)

ABSTRACT

Salidroside (Sal), the main bioactive substance in *Rhodiola rosea*, is a promising functional food component with a wide range of pharmacological effects, but its biological activity is challenging to sustain due to its short half-life, low oral bioavailability, and susceptibility to environmental factors. The aim of this study was to investigate the effect of sodium alginate (SA) concentration on the construction of W/O/W emulsion in the protection of Sal. With the escalation of SA concentrations, the range of droplet size distribution was smaller and the droplets were more uniform. When the concentration of SA was 2 %, the average droplet size reached 9.1 ± 0.1 μm, and the encapsulation efficiency of Sal was 77.8 ± 1.8 %. Moreover, the double emulsion with 2 % SA was the most stable for 28 days at 4 °C since the oil droplets were embedded in the network structure of SA.

1. Introduction

Phenolic compounds are secondary metabolites of plants and have a widespread distribution. They are widely distributed in vegetables, fruits, and other higher plant organs, and play important roles in the aspects of anti-oxidation, anti-cancer, anti-bacteria, and other activities (Khoshnoudi-Nia, Sharif, & Jafari, 2020). Nevertheless, the stability and bioavailability of phenolic compounds are susceptible to environmental factors, which hinders the optimal manifestation of their biological effects on the human body, and limits their application in the food industry (Khoshnoudi-Nia et al., 2020). Therefore, the establishment of food-grade delivery systems for the preservation and conveyance of phenolic compounds has generated considerable attention. For the delivery of hydrophobic phenolic compounds, improving solubility and bioavailability are crucial factors (Markovic et al., 2020). Although sensitive hydrophilic phenolic compounds have high solubility, they face the problems of poor permeability and low bioavailability (Gamboa et al., 2020). Therefore, it is also necessary to construct delivery systems for sensitive hydrophilic phenolic compounds.

Salidroside (Sal) is a water-soluble natural phenolic compound that widely exists in *Rhodiola rosea*. Studies have shown that Sal possesses antioxidant, anti-inflammatory (Zhu, Zhang, Liu, Shi, & Gu, 2016), and anticancer functions (Shang et al., 2019). Although Sal has attractive biological activities, its application in food is severely limited due to its short biological half-life, low oral bioavailability, and sensitivity to temperature, pH, and other environmental factors (Peng et al., 2013). Moreover, in previous studies, liposomes have been extensively studied as delivery systems for Sal, offering targeted delivery therapy (Zhao et al., 2013), while another commonly used delivery system for Sal is hydrogel, which serves as a wound excipient (Peng et al., 2014), and nanoparticles have also been developed for Sal delivery (Fang et al., 2014). However, the development of edible delivery systems for Sal presents significant challenges, which lies in ensuring that all materials used are food-grade and possess adequate physical and chemical stability under the conditions commonly found in the food industry.

W/O/W emulsions are considered suitable components for functional products due to their ability to facilitate the preparation of low-calorie products and provide encapsulation and protection for water-soluble compounds in the inner water phase during digestion. Compared with the existing Sal delivery systems studied previously, most of these systems are used in the medical industry, the development of edible delivery systems for Sal presents significant challenges. Meanwhile, the construction of Sal W/O/W emulsion might be beneficial for the development of low-fat food without changing the original

* Corresponding authors at: College of Food Science and Engineering, Jilin University, Changchun, Jilin 130062, China (B.-W. Zhu); SKL of Marine Food Processing & Safety Control, National Engineering Research Center of Seafood, Collaborative Innovation Center of Seafood Deep Processing, School of Food Science and Technology, Dalian Polytechnic University, Dalian 116034, China (H.-T. Wu).
E-mail addresses: wht205@163.com (H.-T. Wu), zhubeiwei@163.com (B.-W. Zhu).

https://doi.org/10.1016/j.fochx.2024.101260
Received 23 January 2024; Received in revised form 26 February 2024; Accepted 27 February 2024
Available online 29 February 2024

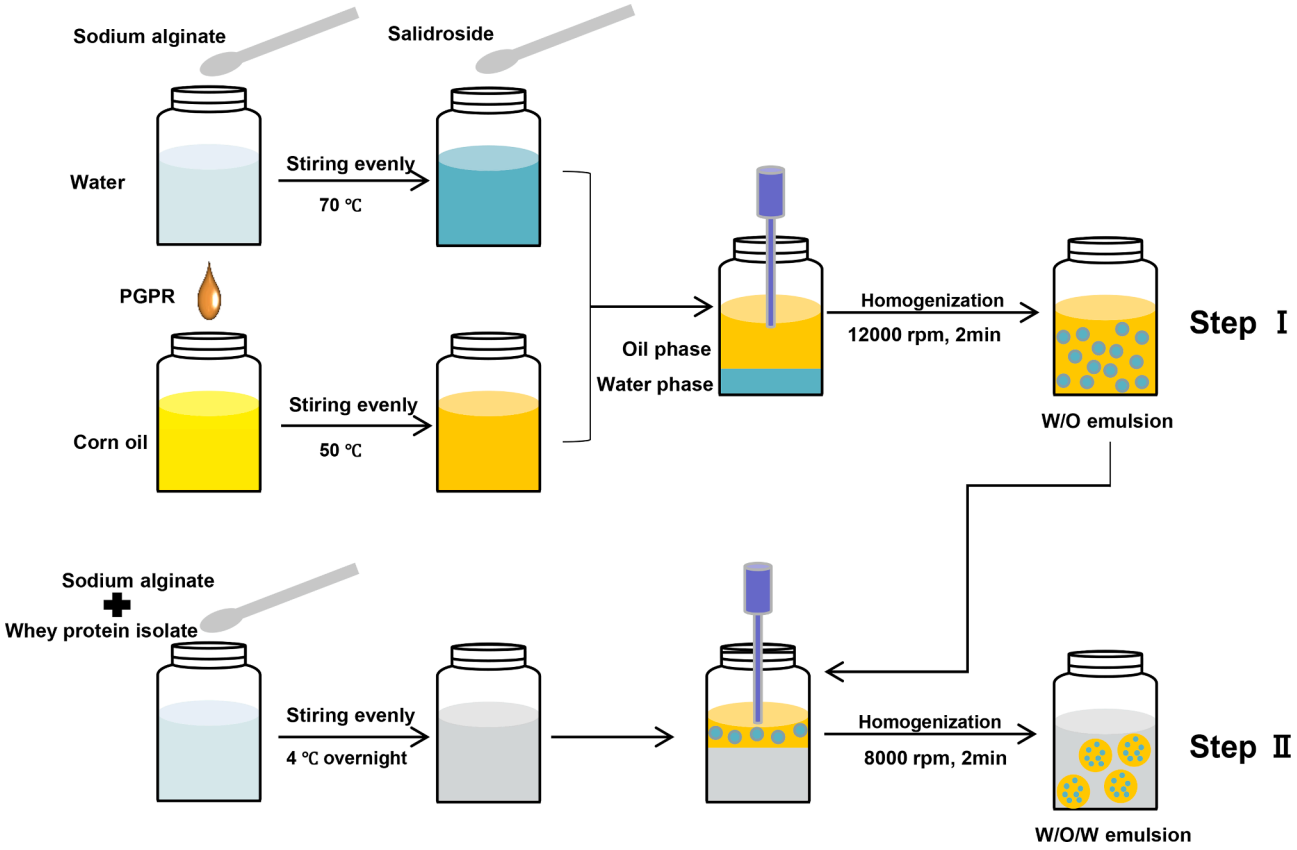

Fig. 1. Flowchart for the preparation of Sal W/O/W emulsions with SA in the outer water phase by two-step method.

flavor of the food matrix (Klojdová & Stathopoulos, 2022). At present, there have been several studies on the preparation of W/O/W emulsions to achieve the encapsulation of hydrophilic active substances, such as caffeic acid, vitamin B_{12}, and anthocyanidin-rich extracts from *Hibiscus Sabdariffa* (Li et al., 2021; Pimentel-Moral, Ochando-Pulido, Segura-Carretero, & Martinez-Ferez, 2018; Raviadaran, Ng, Manickam, & Chandran, 2020), providing a theoretical basis for our research.

The main technologies involved in the preparation of W/O/W emulsions are high-speed shearing, high-pressure homogenization, membrane emulsification, microfluidization, and (ultra)sonication (Muschiolik & Dickinson, 2017). The method includes primary and secondary stages for stabilizing the combination of double emulsion and hydrophilic-hydrophobic particles. The initial step entails preparing W/O emulsions utilizing hydrophobic particles, polyglycerol polyricinoleate (PGPR), sorbitan monolaurate, and sorbitan monooleate, which are often used as oligomer emulsifiers in W/O emulsions (Kawakatsu, Tragardh, & Tragardh, 2001). Among them, PGPR is the most commonly used stabilizer in W/O/W emulsions owing to its remarkable emulsification efficiency, allowing it to be used in the food matrix. While the subsequent step involves generating a double emulsion by blending a single emulsion with an aqueous suspension of hydrophilic particles, hydrophilic emulsifiers such as whey protein isolate (WPI), bovine serum albumin, sodium alginate (SA), xanthan, and acacia gum are commonly utilized in the preparation of W/O/W emulsions (Dickinson, 2011). Among them, SA has gained significant attention in the realm of drug delivery systems owing to its favorable characteristics, including biocompatibility, water solubility, biodegradability, cost-effectiveness and widespread availability (Benegra, Couto, & Pagnoncelli, 2023). Meanwhile, WPI is usually used as carrier material for encapsulating individual and multiple nutrientsm can interact with polysaccharides, enabling the formation of emulsions and this incorporation can enhance protection of bioactive nutrients compared to singular polymers (Chen et al., 2022). Furthermore, previous study demonstrated that SA was best suited for constructing W/O/W emulsion to protect hydrophilic phycocyanin compared with pectin and arabic gum (Teixé-Roig, Oms-Oliu, Ballesté-Muñoz, Odriozola-Serrano, & Martín-Belloso, 2022). However, the application of SA in the construction of Sal W/O/W emulsions has not been studied. Therefore, it is of great significance to study the effect of SA on the construction of Sal W/O/W emulsion.

This study aimed to prepare Sal W/O/W emulsions and investigate the impact of incorporating SA into the outer water phase on the properties of emulsions, including the encapsulation efficiency (EE) of Sal, rheological behavior, moisture distribution, microstructure, and storage stability, which were investigated by fourier transform infrared (FTIR) spectroscopy, rheology tests, low field-nuclear magnetic resonance (LF-NMR) relaxometry, fluorescence inverted microscopy, and cryo-scanning electron microscopy (cryo-SEM). The results showed that 2 % SA had the best effect on the encapsulation of Sal.

2. Materials and methods

2.1. Materials

Sal was procured from Shanghai Maclin Biochemical Technology Co., Ltd. (Shanghai, China). SA (viscosity 200 ± 20 mpa.s) was provided by Shanghai Aladdin Biochemical Technology Co., Ltd. (Shanghai, China). WPI was obtained from Shanghai Yuanye Biotechnology Co. Ltd. (Shanghai, China). Corn oil was provided by Jiusan Grain and Oil Industry Group Co., Ltd. (Harbin, China). PGPR was purchased from Shandong Yousuo Chemical Technology Co., Ltd. (Shandong, China). All other reagents utilized were of analytical grade.

2.2. Preparation of Sal W/O/W emulsion

The two-step emulsification method by high-speed shearing was

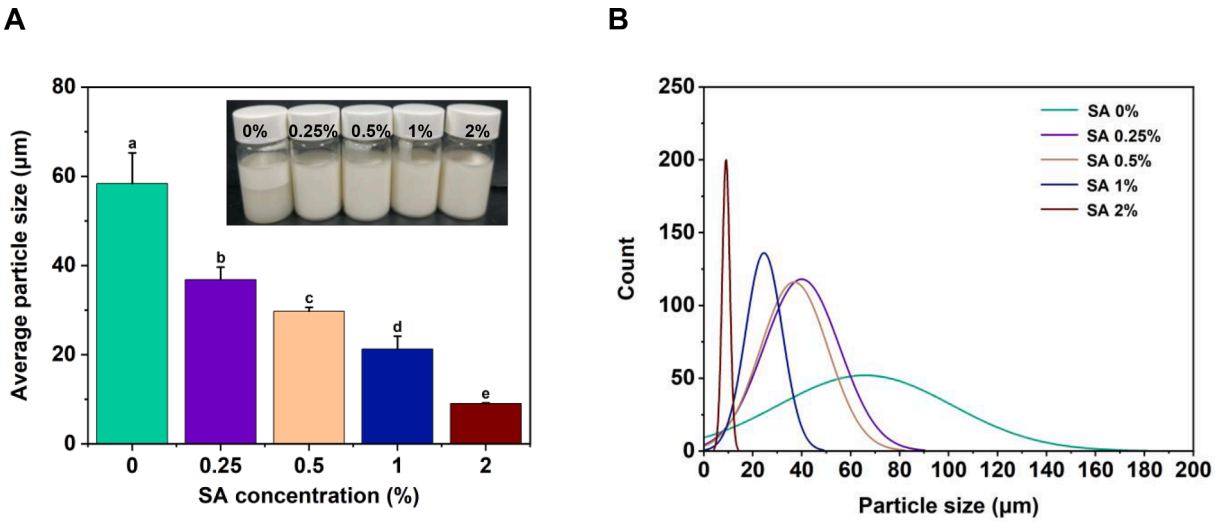

Fig. 2. Appearance and particle size of Sal W/O/W emulsions with different concentrations of SA. (A) Appearance and average particle size of each emulsion; (B) Particle size distribution of each emulsion. SA concentration in the outer water phase of Sal W/O/W emulsions was at 0 %, 0.25%, 0.5 %, 1 %, and 2 %, respectively. Different letters (a–e) indicated significant differences ($p < 0.05$).

used for preparing the Sal W/O/W emulsion due to its high entrapment efficiency and good repeatability. The process involved in preparing the emulsion is shown in Fig. 1. The extent of shear generated by high-shear devices influences the stability of double emulsions. A high shear rate is necessary for creating the primary emulsion, whereas a low shear rate is utilized for dispersing the primary emulsion to prevent disruption of the double emulsion structure (Lamba, Sathish, & Sabikhi, 2015). The initial stage involved the preparation of the primary emulsion, the inner water phase was combined with 1 % (*w/v*) Sal and 2 % (*w/v*) SA, and the corn oil was combined with 4.5 % (*w/w*) PGPR to create the oil phase. The primary emulsion was formed by shearing 70 % (*w/w*) oil phase and 30 % (*w/w*) inner water phase by a high-speed shearing machine (ULTRA TURRAX T18 digital, IKA, Hamburg, Germany) at 12,000 rpm for 2 min. The outer water phase was a mixture of 4 % (*w/v*) WPI and SA at 0%, 0.25 %, 0.5 %, 1 %, and 2 % (*w/v*). The W/O/W emulsion was prepared by shearing 20 % (*w/w*) primary emulsion and 80 % (*w/w*) outer water phase at 8,000 rpm for 2 min. The pH of each solution prior to making an emulsion was adjusted to 7 with 0.1 M NaOH or HCl.

2.3. Average particle size and particle size distribution

The detection of particle size was described by others (Lee, Tan, Ravanfar, & Abbaspourrad, 2019), 200 droplets were randomly selected to measure the particle size individually using an optical microscope from Nikon Optical Instruments Co., Ltd. (Tokyo, Japan). Then the particle size distribution curve was made, and the average particle size was calculated.

2.4. FTIR spectroscopy

The lyophilized samples were mixed with KBr at a mass ratio of 1:100 (*w/w*). A FTIR spectrometer (PerkinElmer, USA) was used to detect the FTIR spectra from 4000 cm^{-1} to 450 cm^{-1} at room temperature. The total number of scans was 32, and the resolution was 4 cm^{-1}.

2.5. EE detection of Sal

The determination of the Sal level in emulsions was conducted using a method developed by others (Dima & Dima, 2018; Tepsongkroh, Harnsilawat, Maisuthisakul, & Chantrapornchai, 2015) with minor modifications. Briefly, deionized water (pH 7) was used to dilute the emulsion five times, and centrifuged at 600 × g for 30 min. After centrifugation, the aqueous bottom layer was subjected to filtration using 0.22 μm syringe filters provided by Tianjin Jinlong Pharmaceutical Technology Development Co., Ltd. (Tianjin, China) and 1 kDa ultrafiltration centrifuges (Merck, Massachusetts, America) for the removal of oil droplets. The level of Sal within the filtrate was determined by measuring the absorbance at 275 nm using a UV-5200 spectrophotometer from Shanghai Yuanxi Instrument Co., Ltd. (Shanghai, China). Each sample underwent a minimum of three measurements, from which the EE (%) of Sal was determined using the following Eq. (1):

$$EE\ (\%) = (A - A_{Sal})/A \times 100\ \% \quad (1)$$

where A_{Sal} represents the amount of unencapsulated Sal in the outer aqueous and A represents the total amount of Sal added.

2.6. Rheological properties

The rheological properties of emulsion samples were monitored using a Discovery Hybrid Rheometer-2 (DHR-2) from TA Instruments Menu Co., Ltd. (New Castle, USA), which was equipped with a parallel plate of 40 mm in diameter. For the frequency scanning model, the storage modulus G' and loss modulus G'' in the frequency range of 0.1–10 Hz were recorded under 0.16 % strain determined by the oscillating stress scanning model. The experimental temperature was 25 °C, and the gap was 1 mm. The viscosity was measured with shear rates of 0.1–100 s^{-1} at a temperature of 25 °C.

2.7. Moisture distribution

A MesoMR23-060V-1 NMR analyzer from Niumag Analytical Instrument Co., Ltd. (Shanghai, China) was employed to measure the transverse spin–spin relaxation (T_2) data of emulsions at 32 °C with a 22.4 MHz resonance frequency and 0.5 T magnetic field strength. The MultiExp Inv analysis program from Niumag Electric Corporation (Shanghai, China) was used to invert the Carr-Purcell-Meiboom-Gill decay curves to obtain related data dispersion exponential fitting.

2.8. Microstructure

The microstructure of the Sal W/O/W emulsion was observed and imaged by fluorescence inverted microscopy from Nikon Optical Instruments Co., Ltd. (Tokyo, Japan) and SU8010 cryo-SEM (HITACHI, Japan).

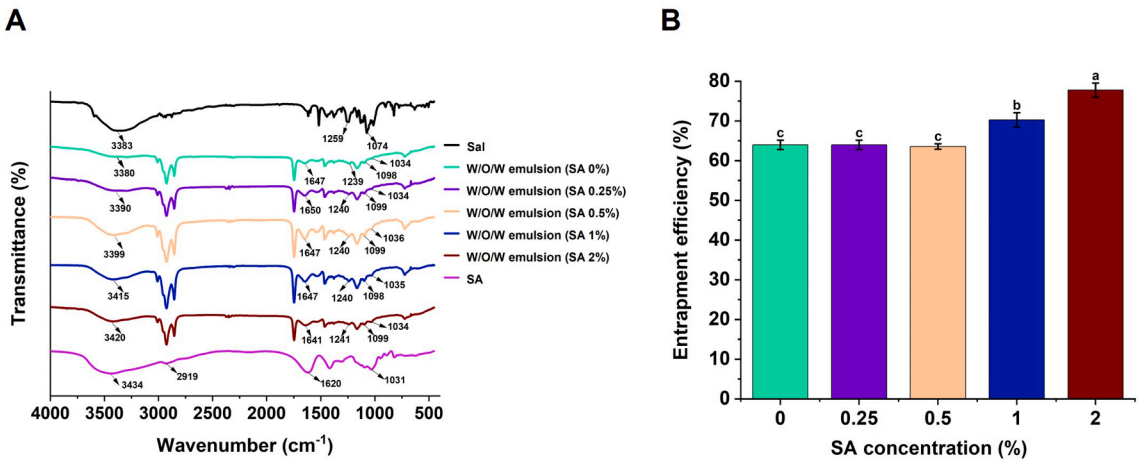

Fig. 3. Sal encapsulation in W/O/W double emulsions with different concentrations of SA. (A) FTIR spectra of Sal W/O/W emulsions freeze-dried powder; (B) EE (%) of Sal in W/O/W emulsions. SA concentration in the outer water phase of Sal W/O/W emulsions was at 0 %, 0.25%, 0.5 %, 1 %, and 2 %, respectively. Different letters (a–c) indicated significant differences ($p < 0.05$).

2.9. Fluorescence staining

Nile red was utilized as a fluorescent dye to label corn oil, while Nile blue was employed to stain WPI in the outer water phase. The staining time was 15 min, and then the samples were observed and imaged by fluorescence inverted microscopy from Nikon Optical Instruments Co., Ltd. (Tokyo, Japan).

2.10. Storage stability

The effect of SA on the storage stability of Sal W/O/W emulsions was investigated, and the emulsions were stored at 4 °C for 28 days to assess their stability during storage. The double emulsions were observed at specific intervals (1, 7, 14, 21, and 28 days), and the particle size was measured using a fluorescence inverted microscopy from Nikon Optical Instruments Co., Ltd. (Tokyo, Japan) at each time point.

2.11. Statistical analyses

All experiments were performed in triplicate. Results are presented as mean ± standard deviation, and statistical analysis was conducted using SPSS 26.0 (IBM, New York, USA). Differences in results were assessed using Duncan's multiple range test at a significance level of $p < 0.05$.

3. Results and discussion

3.1. Appearance and particle size of Sal W/O/W emulsion

Following the emulsion preparation, the emulsion appearance was observed. As shown in Fig. 2A, the emulsions were milky white, based on the fact that the aqueous solutions of Sal and SA were colorless, giving emulsions with the color of WPI. Moreover, when the outer water phase did not contain SA, the emulsion was layered within a few minutes after preparation. After adding SA, the emulsions were homogeneous, which was attributed to the stabilizing function of SA in emulsion systems. The incorporation of anionic SA could augment the emulsifying properties of WPI (Kim, Wang, & Selomulya, 2022) and reduce the osmotic pressure difference between internal and outer water phases, thereby enhancing the emulsion stability and homogenizing the emulsion.

The average particle size and size distribution of the emulsions were further measured. Following preparation, the emulsion was observed under a microscope and photographed. As shown in Fig. 2A and B, the blank emulsion exhibited a unimodal size distribution with a mean diameter of up to 58.6 ± 6.9 μm with the largest particle size distribution range. After adding SA (0.25 %, 0.5 %, 1 %, and 2 %), the average droplet size reached 36.8 ± 2.8, 29.7 ± 0.9, 21.3 ± 2.9, and 9.1 ± 0.1 μm, respectively. This result indicated that with increasing concentrations of SA, the particle size of the Sal emulsion decreased gradually. Since the viscosity of SA with a concentration greater than 2 % is too large, it is difficult to ensure uniformity of the emulsion. In general, the concentration of SA used in the construction of emulsions was 0–2 % (Kim et al., 2022; Mazza et al., 2023). Therefore, the concentration of SA was set at 2 %. At the same time, the particle size distributions were unimodal and the distribution ranges were more centralized. A previous study found there was a gradual reduction in the particle size of egg yolk granule emulsions with the increase in SA, which was consistent with our findings (Zhang et al., 2023). It is possible that the presence of SA promotes a reduction in the initial interfacial tension, which helps the emulsion separate and form droplets with continuous shear stress applied. Thus, smaller and more uniform droplets are produced (Meirelles et al., 2022).

3.2. Sal encapsulation of W/O/W double emulsion

3.2.1. FTIR characterization of Sal W/O/W emulsion

FTIR is a way to analyze the interaction between substances, and is a powerful tool to explore the encapsulation of active substances in the delivery system. The FTIR results of the Sal and emulsions at 4000–450 cm^{-1} are shown in Fig. 3A. As shown in Fig. 3A, the characteristic peaks of Sal were mainly at 3383, 1259, and 1074 cm^{-1}, which were consistent with the previous study (Luo et al., 2015), representing the stretching vibrations associated with —OH, C—O—C, and C—O functional groups, respectively. The peaks observed at 3434, 2919, 1620, and 1031 cm^{-1} in the spectrum of SA correspond to the stretching vibrations of —OH, C—H, —COO—, and C—O—C, respectively (Gao et al., 2023; Mollah, Faruque, Bradley, Khandaker, & Al Assaf, 2023). The stretching vibration of —OH was observed in all emulsions and shifted with the addition of different concentrations of SA, indicating that hydrogen bonding may exert a substantial influence on the formation of double-layer emulsions (Dehkordi, Alemzadeh, Vaziri, & Vossoughi, 2020). Moreover, after the emulsion was formed, the peak intensity at 2919 cm^{-1} of SA disappeared and peak intensity at 1620 cm^{-1} of SA shifted in all emulsions, and the peak at 1259 and 1074 cm^{-1} of Sal disappeared, which indicated that the characteristic peaks of Sal were successfully masked, which further proved the formation of a double-layer emulsion (Zhu, Hu, & Zhong, 2022).

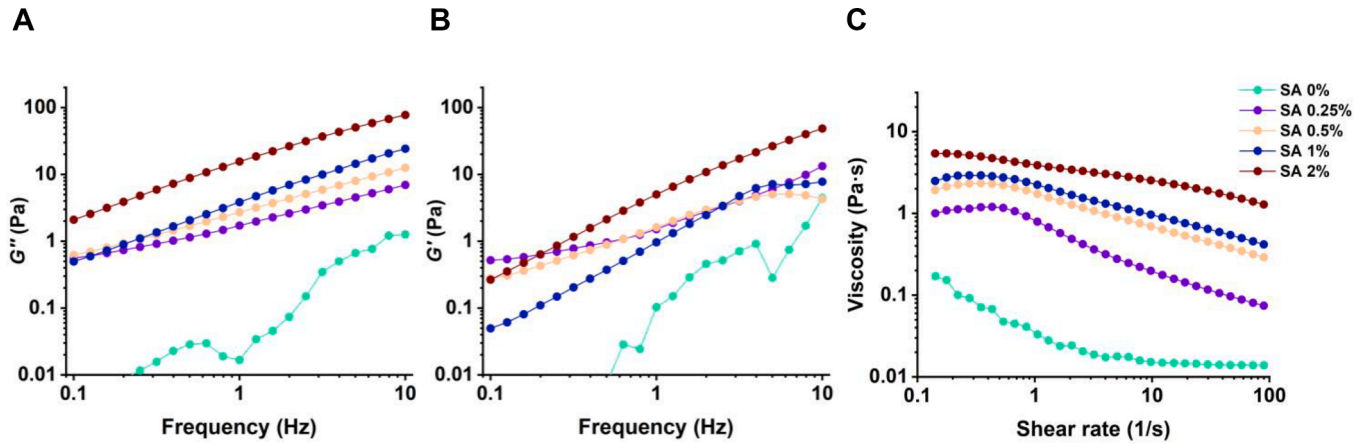

Fig. 4. Rheological properties of Sal W/O/W emulsions with different concentrations of SA. (A) G'' of each emulsion; (B) G' of each emulsion; (C) The viscosity of each emulsion. SA concentration in the outer water phase of Sal W/O/W emulsions was at 0 %, 0.25%, 0.5 %, 1 %, and 2 %, respectively.

3.2.1. EE of Sal in W/O/W emulsion

To confirm the encapsulation of Sal, the EE of Sal in the W/O/W emulsion was detected. As shown in Fig. 3B, where Sal was incorporated into the inner water phase. The EE of Sal increased with increasing doses of SA, indicating that the incorporation of SA mitigated the internal structure disruption of emulsions and minimized the migration of Sal from the inner to outer aqueous phase. The maximal EE of Sal was 77.8 ± 1.8 % when the concentration of SA was 2 %, and this concentration of SA with a higher EE was consistent with a previous study on the encapsulation of nisin (Narsaiah, Jha, Wilson, Mandge, & Manikantan, 2014). The improved EE also suggested that the incorporation of SA improved the stability of the emulsion and mitigated droplet mobility (Chang, Feng, He, Chen, & Liang, 2020). Therefore, the addition of SA made the emulsion difficult to layer after preparation (Fig. 2A). Compared with the Sal delivery system studied previously, the Sal W/O/W emulsion system exhibited a relatively high EE of Sal. For example, the EE of Sal in PLGA-PEG-PLGA nanoparticles was 32.63 ± 0.73 % (Yu et al., 2020), and in niosomes, it was less than 40 % (Zhang et al., 2015). The higher EE of Sal was attributed to the addition of SA, which prevented the migration of Sal to the external aqueous phase. At the same time, the higher EE of Sal in W/O/W emulsion makes the emulsion have the potential to be used as a drug delivery system to improve the therapeutic effect of Sal in the medicine field (Mancuso et al., 2021).

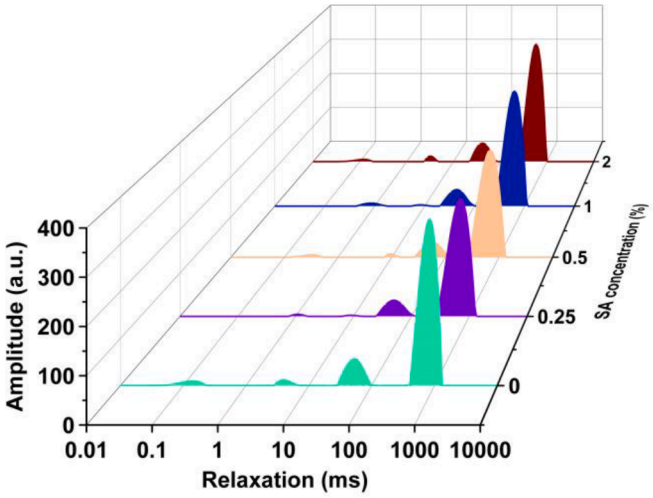

Fig. 5. The T_2 relaxation spectrum of Sal W/O/W emulsions with different concentrations of SA (at 32 °C). SA concentration in the outer water phase of Sal W/O/W emulsions was at 0 %, 0.25%, 0.5 %, 1 %, and 2 %, respectively.

3.3. Rheological characteristics of Sal W/O/W emulsion

To further understand the impact of SA concentrations on the physical properties of the Sal W/O/W emulsion, the storage modulus G' and loss modulus G'' with frequency were tested (Fig. 4A and B). In the frequency range between 0.1 and 10 Hz, G'' values were consistently higher than those of G' in all emulsion samples, which indicated that the system was in a liquid state, and the viscous characteristics were dominant. Moreover, in the presence of SA, all emulsion samples showed frequency-dependent behavior. In addition, with increasing SA concentration, G'' gradually increased, and G' was independent of SA concentration. The increase in the modulus indicated that some structural rearrangement occurred, which was related to the redistribution of the droplet size (Farias et al., 2020). This result was in line with the particle size distribution results (Fig. 2B). Furthermore, when the concentration of SA was 2 %, the increase in G' was more rapid than that in G'', this phenomenon indicated the existence of a gel-like behavior in the emulsion (Yu et al., 2022).

Polysaccharides are commonly employed as stabilizers for the continuous phase to enable emulsification and enhance the stability of emulsions through an increase in viscosity. Hence, the apparent viscosity of the emulsion was measured accordingly (Fig. 4C). The emulsions displayed a consistent rise in viscosity as the concentration of SA increased across the entire range of shear rate variations. It has been reported that the enhancement of emulsion viscosity has a beneficial effect on the stability of emulsions (Lu, Zheng, & Miao, 2018). At the same time, all the samples showed shear thinning behavior, possibly due to the fracture of the aggregation network between the droplets during the shearing process (Li et al., 2021), which indicated that the emulsion samples were non-Newtonian fluids. Under shear rates of 0.1–100 s^{-1}, the emulsion without SA exhibited a viscosity of less than 0.18 Pa·s. When the concentration of SA was 2 %, the viscosity exceeded 5 Pa·s. This may be attributed to the formation of SA network structure in the outer water phase. Additionally, the rise in viscosity led to a decrease in the emulsion particle size, which corresponded to the particle size results in our study described in Fig. 2. The same phenomenon was also found in a previous study in which the higher viscosity of the continuous phase was, the smaller the droplets of the W/O/W emulsion were (Vladisavljevic, Shimizu, & Nakashima, 2006). In addition, the higher EE of Sal in this study (Fig. 3B) can be attributed to the well-established property of SA as a thickening agent. Since the concentration of SA was identified as the primary factor influencing the viscosity of the emulsion, higher emulsion viscosity can mitigate instability by augmenting resistance to coalescence at the same time, and emulsion stability and droplet size in turn directly affect the EE (Mazza et al., 2023). Therefore, in a

Table 1
Relaxation time of Sal W/O/W emulsions.

SA concentration (%)	Relaxation time			
	T_{2b} (ms)	T_{21} (ms)	T_{22} (ms)	T_{23} (ms)
0	0.15 ± 0.01^{b}	3.63 ± 0.76^{b}	57.42 ± 2.27^{a}	841.12 ± 34.09^{a}
0.25	0.71 ± 0.51^{a}	8.98 ± 3.79^{a}	53.57 ± 2.10^{ab}	732.08 ± 29.67^{b}
0.5	0.26 ± 0.10^{ab}	8.46 ± 1.17^{a}	53.65 ± 4.40^{ab}	668.06 ± 46.35^{c}
1	0.66 ± 0.22^{ab}	9.26 ± 1.00^{a}	51.71 ± 9.87^{ab}	652.08 ± 25.83^{c}
2	0.16 ± 0.05^{b}	3.27 ± 0.35^{b}	44.56 ± 3.09^{b}	580.52 ± 0.00^{d}

Data were expressed as mean ± SD, and values followed by different superscript letters in the same column were significantly different ($p < 0.05$). Experiments were performed in triplicate.

certain range of SA concentrations, increasing the viscosity can improve the EE of Sal.

3.4. Moisture distribution of Sal W/O/W emulsion

The water distribution of Sal W/O/W emulsions with various concentrations of SA was determined by LF-NMR. LF-NMR has been extensively employed in investigating proton mobility within protein/polysaccharide gel systems (Li et al., 2020). Fig. 5 and Table 1 showed that the relaxation time of hydrogen protons was assessed by multi-exponential fitting of a T_2 distribution, which identified four peaks in the double-layer emulsions. The four components of relaxation were as follows: T_{2b} (0.1–1 ms) is attributed to the water molecules that are either bound within macromolecular structures or exist as hydration water. T_{21} (1–10 ms) primarily refers to water that is tightly connected to macromolecules or oil present in the gel network, indicating restricted mobility of these molecules. T_{22} (10–100 ms) indicates the water that is immobilized within the gel network. T_{23} (100–10000 ms) can be designated as the free water fraction (Li et al., 2020; Yan et al., 2021). As shown in Fig. 5 and Table 1, more than 91 % of the total signals in all samples were free water, which was identified as a main component of the emulsion. The relatively high water content and low oil content make Sal W/O/W emulsion have the potential to be used as a fat substitute in the food industry. Such as, functional ice cream (Klojdová & Stathopoulos, 2022). With the increase of SA concentration, the peaks at T_{23} in the transverse relaxation spectra of the emulsions exhibited a significant leftward shift, indicating the inhibition of hydrogen proton mobility in water. The variations in T_{2b}, T_{21}, and T_{22} were independent of the dose of SA. Moreover, when the concentration of SA was 2 %, the T_{23} value was the lowest (580.5 ms), indicating that the sample exhibited superior water incorporation ability compared to the other emulsions. This phenomenon could be attributed to the particle size of the emulsion, as the reduced particle size helps the emulsion capture more water (Zhang et al., 2021). The decrease in the T_{23} value indicated that the migration of hydrogen protons in water was inhibited and the emulsion facilitated a more gel-like property (Zhang et al., 2021). The LF-NMR results were consistent with the rheology data mentioned above.

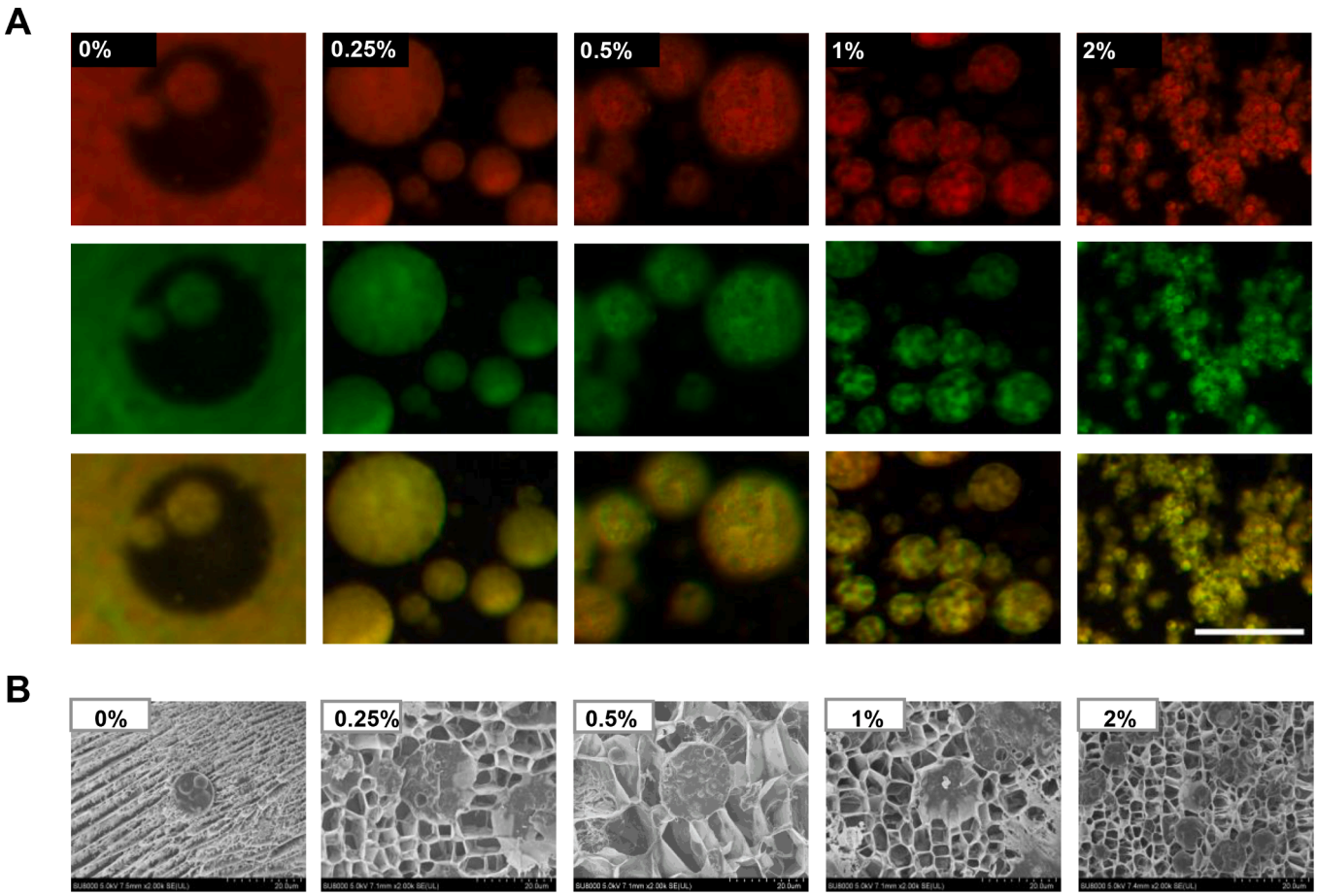

Fig. 6. Microstructure of Sal W/O/W emulsions with different concentrations of SA. (A) Fluorescence staining of each emulsion with a scale bar of 50 μm; (B) Cryo-SEM micrographs of each emulsion with a scale bar of 20 μm. SA concentration in the outer water phase of Sal W/O/W emulsions was at 0 %, 0.25%, 0.5 %, 1 %, and 2 %, respectively.

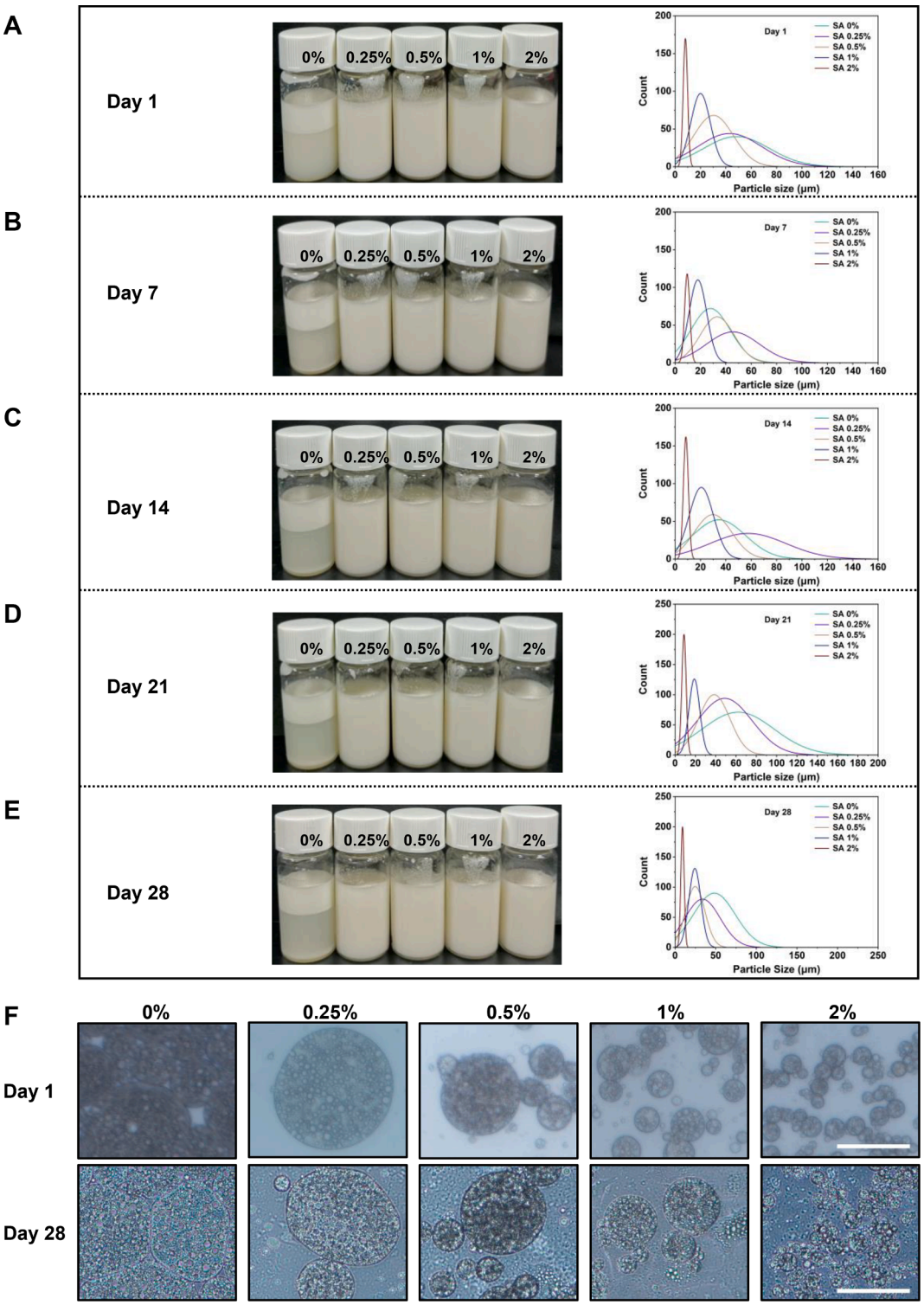

Fig. 7. The storage stability of Sal W/O/W emulsions with different concentrations of SA at 4 °C for 28 days. (A-E) Appearance and size distribution of each emulsion at 1, 7, 14, 21, and 28 days; (F) Optical microscopy images with a scale bar of 50 μm at 1 and 28 days. SA concentration in the outer water phase of Sal W/O/W emulsions was at 0 %, 0.25%, 0.5 %, 1 %, and 2 %, respectively.

3.5. Microstructure of Sal W/O/W emulsion

3.5.1. Fluorescence staining of Sal W/O/W emulsion

In order to verify the formation of the Sal W/O/W emulsion microstructure, the emulsion underwent fluorescence staining. The corn oil was stained with Nile red, while the WPI in the outer water phase was stained with Nile blue. As shown in Fig. 6A, by adding various concentrations of SA (0.25 %, 0.5 %, 1 %, and 2 %), the emulsion droplets gradually formed, and the droplets appeared as regular circles. The overlap of green fluorescence (corn oil) and red fluorescence (WPI) can be clearly observed, which indicated the formation of O/W emulsion (Huang et al., 2021), and the inner water phase inside the oil droplet was not fluorescent (appearing black), which indicated the formation of W/O structure and that the outer water phase did not penetrate into the

inner water phase. Thus, the microstructure of the Sal W/O/W emulsion was established.

3.5.2. Cryo-SEM of Sal W/O/W emulsion

To further illustrate the generation of the double-layer emulsion, the emulsion microstructure was characterized using cryo-SEM (Fig. 6B). The cryo-SEM images suggested that the emulsion particle size was smaller than that observed in Nikon fluorescence inverted microscope images, possibly due to the potential shrinkage during the cryo-SEM preparation procedure. With the increase of SA concentration, the particle size of the emulsion decreased, which was consistent with the results shown in Fig. 2A. As shown in Fig. 6B, in the sample without SA, the oil droplets were poorly covered, and phase delamination occurred. SA was found to significantly alter the microstructure of the emulsion, and the oil droplets were gradually embedded in the network structure of SA. SA effectively covering the surface of the droplets can reduce the surface tension, impede oil droplets accumulation, and improve droplets stability. When the concentration of SA was 2 %, the droplets formed a denser three-dimensional network space structure, and this structural characteristic of the Sal W/O/W emulsion played a role in enhancing system stability.

3.6. Effect of SA content on the storage stability of Sal W/O/W emulsions

The impact of SA concentration on the storage stability of the Sal W/O/W system was investigated. The double emulsion was observed at 1, 7, 14, 21, and 28 days, and the particle size was measured at every time interval (Fig. 7). After 1 day of storage, the double emulsion lacking SA exhibited significant creaming, as depicted in Fig. 7A. This phenomenon could be attributed to the relatively large droplet size and low viscosity of the WPI-stabilized emulsion. Moreover, the addition of SA greatly enhanced the stability of the emulsion, effectively preventing creaming. The principal factors contributing to emulsion instability are low viscosity and high interfacial tension (Lee et al., 2019). Adding SA to the emulsion can increase the viscosity and decrease oil droplet movement and accumulation, thereby enhancing the stability of the system. For example, the addition of SA could improve the stabilization of W/O emulsions (Tepsongkroh et al., 2015). The droplet size distributions with varying concentrations of SA in the double emulsion at 4 °C for 28 days are illustrated in Fig. 7A–E. In combination with the microscopic observation of the emulsion state (Fig. 7F), it was observed that the double layer structure of the emulsion was always present in each sample with SA addition, and the structure was consistent with the fluorescence staining result described in Fig. 6A. This may be because the SA can function as a texture modifier in the aqueous phase to improve emulsion stability by impeding droplet movement. This result was achieved through their ability to interact with surfactant chains surrounding oil droplets, resulting in steric and/or electrostatic repulsion between droplet interfaces and preventing destabilization phenomena such as coalescence or gravitational separation. For example, it has been reported that globular proteins can interact with SA in aqueous solutions to form soluble or insoluble complexes to stabilize the system (Sosa-Herrera, Lozano-Esquivel, de Leon-Ramirez, & Martinez-Padilla, 2012). Moreover, SA increased the emulsion viscosity and facilitated the formation of smaller droplets, thereby impeding emulsion creaming (Yu et al., 2022). And adequate alginate molecules were available to fully saturate the surfaces of the droplets preventing flocculation of the droplets. Therefore, SA could increase the emulsion stability. Remarkably, the emulsion system formed by 2 % SA exhibited the smallest particle size and highest stability. Simultaneously, the addition of SA increased the viscosity and EE of Sal (Fig. 3B). The EE is strongly influenced by the physical stability, and emulsions with poor physical stability usually exhibit significantly low EE (Santos, Trujillo-Cayado, Barquero, & Calero, 2022). This also proved that the addition of SA could improve the storage stability of the Sal W/O/W emulsion. In addition, to enhance stability, internal water phase can be gelled, resulting in the formation of a gel-in-oil-in-water emulsion, which is a potential system for encapsulating Sal (Perez-Moral, Watt, & Wilde, 2014).

4. Conclusions

In summary, Sal W/O/W emulsions stabilized by WPI, SA, and PGPR were conducted with the double layer structure. SA was positively correlated with the stability and EE of Sal W/O/W emulsions in a concentration range from 0 to 2 %. Structurally, the oil droplets are wrapped into the shell structure of SA, which can protect the oil droplets from coalescing and improve the storage stability of the emulsion. SA increased the continuous phase viscosity and water incorporation ability can also contribute to the Sal W/O/W emulsion stability. This study provides a theoretical basis and scientific support for the application of Sal in food and medicine fields. In the future, the *in vivo* performance will be studied to assess the pharmacologically beneficial impacts of Sal W/O/W emulsion and different emulsifier combinations for constructing Sal W/O/W emulsions will be explored.

CRediT authorship contribution statement

Qian Zhang: Writing – original draft, Validation, Methodology, Investigation, Formal analysis, Data curation, Conceptualization. **Yu-Qiao Wang:** Investigation. **Lin Li:** Investigation. **Hao-Lin Song:** Investigation. **Hai-Tao Wu:** Writing – review & editing, Supervision, Project administration, Funding acquisition. **Bei-Wei Zhu:** Writing – review & editing, Supervision, Project administration, Funding acquisition.

Declaration of competing interest

The authors declare that they have no known competing financial interests or personal relationships that could have appeared to influence the work reported in this paper.

Data availability

The data that has been used is confidential.

Acknowledgment

This work was supported by the Science and Technology Program of Liaoning Province (2022JH1/10900010).

References

Benegra, M., Couto, G. H., & Pagnoncelli, M. G. B. (2023). Preparation and evaluation of w/o/w-type emulsions for encapsulation of citronella essential oil by inverse ionic gelation. *Colloid and Polymer Science, 301*(10), 1159–1170. https://doi.org/10.1007/s00396-023-05134-w

Chang, X., Feng, W. W., He, L., Chen, X., & Liang, L. (2020). Fabrication and characterisation of whey protein isolate-propolis-alginate complex particles for stabilising alpha-tocopherol-contained emulsions. *International Dairy Journal, 109*. https://doi.org/10.1016/j.idairyj.2020.104756

Chen, W. J., Wang, W. J., Guo, M. M., Li, Y. C., Meng, F. B., & Liu, D. H. (2022). Whey protein isolate-gum Acacia Maillard conjugates as emulsifiers for nutraceutical emulsions: Impact of glycation methods on physicochemical stability and in vitro bioaccessibility of 13-carotene emulsions. *Food Chemistry, 375*. https://doi.org/10.1016/j.foodchem.2021.131706

Dehkordi, S. S., Alemzadeh, I., Vaziri, A. S., & Vossoughi, A. (2020). Optimization of alginate-whey protein isolate microcapsules for survivability and release behavior of probiotic bacteria. *Applied Biochemistry and Biotechnology, 190*(1), 182–196. https://doi.org/10.1007/s12010-019-03071-5

Dickinson, E. (2011). Double emulsions stabilized by food biopolymers. *Food Biophysics, 6*(1), 1–11. https://doi.org/10.1007/s11483-010-9188-6

Dima, C., & Dima, S. (2018). Water-in-oil-in-water double emulsions loaded with chlorogenic acid: Release mechanisms and oxidative stability. *Journal of Microencapsulation, 35*(6), 584–599. https://doi.org/10.1080/02652048.2018.1559246

Fang, D. L., Chen, Y., Xu, B., Ren, K., He, Z. Y., He, L. L., et al. (2014). Development of lipid-shell and polymer core nanoparticles with water-soluble salidroside for anti-

cancer therapy. *International Journal of Molecular Sciences, 15*(3), 3373–3388. https://doi.org/10.3390/ijms15033373
Farias, B. V., Brown, D., Hearn, A., Nunn, N., Shenderova, O., & Khan, S. A. (2020). Nanodiamond-stabilized Pickering emulsions: Microstructure and rheology. *Journal of Colloid and Interface Science, 580*, 180–191. https://doi.org/10.1016/j.jcis.2020.07.030
Gamboa, A., Schussler, N., Soto-Bustamante, E., Romero-Hasler, P., Meinel, L., & Morales, J. O. (2020). Delivery of ionizable hydrophilic drugs based on pharmaceutical formulation of ion pairs and ionic liquids. *European Journal of Pharmaceutics and Biopharmaceutics, 156*, 203–218. https://doi.org/10.1016/j.ejpb.2020.09.007
Gao, Y. J., Jin, W. J., Liu, S. F., Cheng, X. W., Guan, J. P., & Yang, X. H. (2023). Flame retardancy and combustion performance of polysaccharide fabrics: A comparison on cotton and calcium alginate fabrics. *Polymer Testing, 124*. https://doi.org/10.1016/j.polymertesting.2023.108099
Huang, Z., Guo, B., Deng, C., Tang, C., Liu, C., & Hu, X. (2021). Fabrication and characterization of the W/O/W multiple emulsion through oleogelation of oil. *Food Chemistry, 358*, Article 129856. https://doi.org/10.1016/j.foodchem.2021.129856
Kawakatsu, T., Tragardh, G., & Tragardh, C. (2001). Production of W/O/W emulsions and S/O/W pectin microcapsules by microchannel emulsification. *Colloids and Surfaces A-Physicochemical and Engineering Aspects, 189*(1–3), 257–264. https://doi.org/10.1016/s0927-7757(01)00508-8
Khoshnoudi-Nia, S., Sharif, N., & Jafari, S. M. (2020). Loading of phenolic compounds into electrospun nanofibers and electrosprayed nanoparticles. *Trends in Food Science & Technology, 95*, 59–74. https://doi.org/10.1016/j.tifs.2019.11.013
Kim, W., Wang, Y., & Selomulya, C. (2022). Impact of sodium alginate on binary whey/pea protein-stabilised emulsions. *Journal of Food Engineering, 321*. https://doi.org/10.1016/j.jfoodeng.2022.110978
Klojdová, I., & Stathopoulos, C. (2022). W/o/w multiple emulsions: A novel trend in functional ice cream preparations? *Food Chemistry-X, 16*. https://doi.org/10.1016/j.fochx.2022.100451
Lamba, H., Sathish, K., & Sabikhi, L. (2015). Double emulsions: Emerging delivery system for plant bioactives. *Food and Bioprocess Technology, 8*(4), 709–728. https://doi.org/10.1007/s11947-014-1468-6
Lee, M. C., Tan, C., Ravanfar, R., & Abbaspourrad, A. (2019). Ultrastable water-in-oil high internal phase emulsions featuring interfacial and biphasic network stabilization. *ACS Applied Materials & Interfaces, 11*(29), 26433–26441. https://doi.org/10.1021/acsami.9b05089
Li, L. J., He, M. Y., Yang, H. D., Wang, N., Kong, Y., Li, Y., et al. (2021). Effect of soybean lipophilic protein-methyl cellulose complex on the stability and digestive properties of water-in-oil-in-water emulsion containing vitamin B-12. *Colloids and Surfaces A-Physicochemical and Engineering Aspects, 629*. https://doi.org/10.1016/j.colsurfa.2021.127364
Li, J. H., Xu, L. L., Su, Y. J., Chang, C. H., Yang, Y. J., & Cu, L. P. (2020). Flocculation behavior and gel properties of egg yolk/kappa-carrageenan composite aqueous and emulsion systems: Effect of NaCl. *Food Research International, 132*. https://doi.org/10.1016/j.foodres.2020.108990
Lu, W., Zheng, B. D., & Miao, S. (2018). Improved emulsion stability and modified nutrient release by structuring O/W emulsions using konjac glucomannan. *Food Hydrocolloids, 81*, 120–128. https://doi.org/10.1016/j.foodhyd.2018.02.034
Luo, M., Peng, H. L., Deng, Z. H., Yin, Z. H., Zhao, Q., & Xiong, H. (2015). Preparation and characterization of genipin-crosslinked chitosan microspheres for the sustained release of salidroside. *International Journal of Food Engineering, 11*(3), 323–333. https://doi.org/10.1515/ijfe-2014-0314
Mancuso, A., Cristiano, M. C., Pandolfo, R., Greco, M., Fresta, M., & Paolino, D. (2021). Improvement of ferulic acid antioxidant activity by multiple emulsions: In vitro and in vivo evaluation. *Nanomaterials, 11*(2). https://doi.org/10.3390/nano11020425
Markovic, M. D., Panic, V. V., Seslija, S. I., Milivojevic, A. D., Spasojevic, P. M., Boskovic-Vragolovic, N. M., et al. (2020). Novel strategy for encapsulation and targeted delivery of poorly water-soluble active substances. *Polymer Engineering and Science, 60*(8), 2008–2022. https://doi.org/10.1002/pen.25448
Mazza, K. E. L., Costa, A. M. M., Silva, J. P. L. D., Alviano, D. S., Bizzo, H. R., & Tonon, R. V. (2023). Microencapsulation of marjoram essential oil as a food additive using sodium alginate and whey protein isolate. *International Journal of Biological Macromolecules, 233*. https://doi.org/10.1016/j.ijbiomac.2023.123478
Meirelles, A. A. D., Costa, A. L. R., Michelon, M., Vigano, J., Carvalho, M. S., & Cunha, R. L. (2022). Microfluidic approach to produce emulsion-filled alginate microgels. *Journal of Food Engineering, 315*. https://doi.org/10.1016/j.jfoodeng.2021.110812
Mollah, M. Z. I., Faruque, M. R. I., Bradley, D. A., Khandaker, M. U., & Al Assaf, S. (2023). FTIR and rheology study of alginate samples: Effect of radiation. *Radiation Physics and Chemistry, 202*. https://doi.org/10.1016/j.radphyschem.2022.110500
Muschiolik, G., & Dickinson, E. (2017). Double emulsions relevant to food systems: Preparation, stability, and applications. *Comprehensive Reviews in Food Science and Food Safety, 16*(3), 532–555. https://doi.org/10.1111/1541-4337.12261
Narsaiah, K., Jha, S. N., Wilson, R. A., Mandge, H. M., & Manikantan, M. R. (2014). Optimizing microencapsulation of nisin with sodium alginate and guar gum. *Journal of Food Science and Technology, 51*(12), 4054–4059. https://doi.org/10.1007/s13197-012-0886-6
Peng, H., Dong, R., Wang, S., Zhang, Z., Luo, M., Bai, C., et al. (2013). A pH-responsive nano-carrier with mesoporous silica nanoparticles cores and poly(acrylic acid) shell-layers: Fabrication, characterization and properties for controlled release of salidroside. *International Journal of Pharmaceutics, 446*(1–2), 153–159. https://doi.org/10.1016/j.ijpharm.2013.01.071
Peng, L. H., Xu, S. Y., Shan, Y. H., Wei, W., Liu, S., Zhang, C. Z., et al. (2014). Sequential release of salidroside and paeonol from a nanosphere-hydrogel system inhibits ultraviolet B-induced melanogenesis in Guinea pig skin. *International Journal of Nanomedicine, 9*, 1897–1908. https://doi.org/10.2147/IJN.S59290
Perez-Moral, N., Watt, S., & Wilde, P. (2014). Comparative study of the stability of multiple emulsions containing a gelled or aqueous internal phase. *Food Hydrocolloids, 42*, 215–222. https://doi.org/10.1016/j.foodhyd.2014.05.023
Pimentel-Moral, S., Ochando-Pulido, J. M., Segura-Carretero, A., & Martinez-Ferez, A. (2018). Stabilization of W/O/W multiple emulsion loaded with Hibiscus sabdariffa extract through protein-polysaccharide complexes. *LWT-Food Science and Technology, 90*, 389–395. https://doi.org/10.1016/j.lwt.2017.12.054
Raviadaran, R., Ng, M. H., Manickam, S., & Chandran, D. (2020). Ultrasound-assisted production of palm oil-based isotonic W/O/W multiple nanoemulsion encapsulating both hydrophobic tocotrienols and hydrophilic caffeic acid with enhanced stability using oil-based sucragel. *Ultrasonics Sonochemistry, 64*. https://doi.org/10.1016/j.ultsonch.2020.104995
Santos, J., Trujillo-Cayado, L. A., Barquero, M., & Calero, N. (2022). Influence of type and concentration of biopolymer on beta-carotene encapsulation efficiency in nanoemulsions based on linseed oil. *Polymers (Basel), 14*(21). https://doi.org/10.3390/polym14214640
Shang, H., Wang, S., Yao, J., Guo, C., Dong, J., & Liao, L. (2019). Salidroside inhibits migration and invasion of poorly differentiated thyroid cancer cells. *Thorac Cancer, 10*(6), 1469–1478. https://doi.org/10.1111/1759-7714.13096
Sosa-Herrera, M. G., Lozano-Esquivel, I. E., de Leon-Ramirez, R. P., & Martinez-Padilla, L. P. (2012). Effect of added calcium chloride on the physicochemical and rheological properties of aqueous mixtures of sodium caseinate/sodium alginate and respective oil-in-water emulsions. *Food Hydrocolloids, 29*(1), 175–184. https://doi.org/10.1016/j.foodhyd.2012.02.017
Teixé-Roig, J., Oms-Oliu, G., Balleste-Muñoz, S., Odriozola-Serrano, I., & Martín-Belloso, O. (2022). Encapsulation and controlled release of phycocyanin during the in vitro digestion using polysaccharide-added double emulsions (W1/O/W2). *Food Structure-Netherlands, 31*. https://doi.org/10.1016/j.foostr.2021.100249
Tepsongkroh, B., Harnsilawat, T., Maisuthisakul, P., & Chantrapornchai, W. (2015). Influence of polyglycerol polyricinoleate and biopolymers on physical properties and encapsulation efficiency of water-in-oil-in-water emulsions containing mango seed kernel extract. *Journal of Dispersion Science and Technology, 36*(8), 1126–1133. https://doi.org/10.1080/01932691.2014.956116
Vladisavljevic, G. T., Shimizu, M., & Nakashima, T. (2006). Production of multiple emulsions for drug delivery systems by repeated SPG membrane homogenization: Influence of mean pore size, interfacial tension and continuous phase viscosity. *Journal of Membrane Science, 284*(1–2), 373–383. https://doi.org/10.1016/j.memsci.2006.08.003
Yan, J. N., Du, Y. N., Jiang, X. Y., Han, J. R., Pan, J. F., & Wu, H. T. (2021). Intermolecular interaction in the hybrid gel of scallop (Patinopecten yessoensis) male gonad hydrolysates and kappa-carrageenan. *Journal of Food Science, 86*(3), 792–802. https://doi.org/10.1111/1750-3841.15618
Yu, X., Sun, L. L., Tan, L. J., Wang, M., Ren, X. L., Pi, J. X., et al. (2020). Preparation and characterization of PLGA-PEG-PLGA nanoparticles containing salidroside and tamoxifen for breast cancer therapy. *AAPS PharmSciTech, 21*(3). https://doi.org/10.1208/s12249-019-1523-8
Yu, H. J., Wang, H. T., Su, W. T., Song, Y. K., Zaky, A. A., Abd El-Aty, A. M., et al. (2022). Co-delivery of hydrophobic astaxanthin and hydrophilic phycocyanin by a pH-sensitive water-in-oil-in-water double emulsion-filled gellan gum hydrogel. *Food Hydrocolloids, 131*. https://doi.org/10.1016/j.foodhyd.2022.107810
Zhang, X., Chen, X., Gong, Y. H., Li, Z. Y., Guo, Y. F., Yu, D. A. Y., et al. (2021). Emulsion gels stabilized by soybean protein isolate and pectin: Effects of high intensity ultrasound on the gel properties, stability and 13-carotene digestive characteristics. *Ultrasonics Sonochemistry, 79*. https://doi.org/10.1016/j.ultsonch.2021.105756
Zhang, H., Tan, S. M., Gan, H. M., Zhang, H. J., Xia, N., Jiang, L. W., et al. (2023). Investigation of the formation mechanism and beta-carotene encapsulation stability of emulsion gels based on egg yolk granules and sodium alginate. *Food Chemistry, 400*. https://doi.org/10.1016/j.foodchem.2022.134032
Zhang, Y., Zhang, K., Wu, Z., Guo, T., Ye, B., Lu, M., et al. (2015). Evaluation of transdermal salidroside delivery using niosomes via in vitro cellular uptake. *International Journal of Pharmaceutics, 478*(1), 138–146. https://doi.org/10.1016/j.ijpharm.2014.11.018
Zhao, X., Lu, Y., Tao, Y., Huang, Y., Wang, D., Hu, Y., et al. (2013). Salidroside liposome formulation enhances the activity of dendritic cells and immune responses. *International Immunopharmacology, 17*(4), 1134–1140. https://doi.org/10.1016/j.intimp.2013.10.016
Zhu, Z., Hu, J., & Zhong, Z. (2022). Preparation and characterization of long-term antibacterial and pH-responsive polylactic acid/octenyl succinic anhydride-chitosan @ tea tree oil microcapsules. *International Journal of Biological Macromolecules, 220*, 1318–1328. https://doi.org/10.1016/j.ijbiomac.2022.09.038
Zhu, Y., Zhang, Y. J., Liu, W. W., Shi, A. W., & Gu, N. (2016). Salidroside suppresses HUVECs cell injury induced by oxidative stress through activating the Nrf2 signaling pathway. *Molecules, 21*(8). https://doi.org/10.3390/molecules21081033